

Supporting Information

Lipid vesicle composition influences the incorporation and fluorescence properties of the lipophilic sulphonated carbocyanine dye SP-DiO

Quentin Lubart^{1,2}, Jonas Hannestad¹, Hudson Pace³, Daniel Fjällborg¹, Fredrik Westerlund², Elin K. Esbjörner², Marta Bally^{4*}

¹Division of Biological Physics, Department of Physics, Chalmers University of Technology, 41296 Gothenburg, Sweden

²Division of Chemical Biology, Department of Biology and Biological Engineering, Chalmers University of Technology, 41296 Gothenburg, Sweden

³ Department of Integrative Medical Biology, Umeå University, 90185 Umeå, Sweden

⁴ Department of Clinical Microbiology & Wallenberg Centre for Molecular Medicine, Umeå University, 90185 Umeå, Sweden.

*corresponding author: marta.bally@umu.se

S1. Spectral properties of the dye in different lipid environments

The spectral properties of the SP-DiO dye in different lipid environments were determined by fluorimetry as described in the materials and methods section (section 2.5) of the manuscript. The obtained excitation and emission peaks are reported in Table S1.

Table S1. Spectral properties of SP-DiO C18(3) in different lipid environments

Formulations	λ_{ex} [nm]	λ_{em} [nm]
DOPS	501 ± 1	517 ± 1
DOPC	501 ± 0	517 ± 1
POPC	501 ± 0	517 ± 1
DSPC	503 ± 1	517 ± 1
DPPC	507 ± 4	519 ± 1
DMPC	503 ± 1	516 ± 1
POPC/Chol 9/1	501 ± 0	517 ± 1
POPC/Chol 7/3	504 ± 1	542 ± 0

A normalization of the absorption and emission spectra allows for a comparison of the spectra profiles for the dye in different lipid environments (Figure S1 and Figure S2).

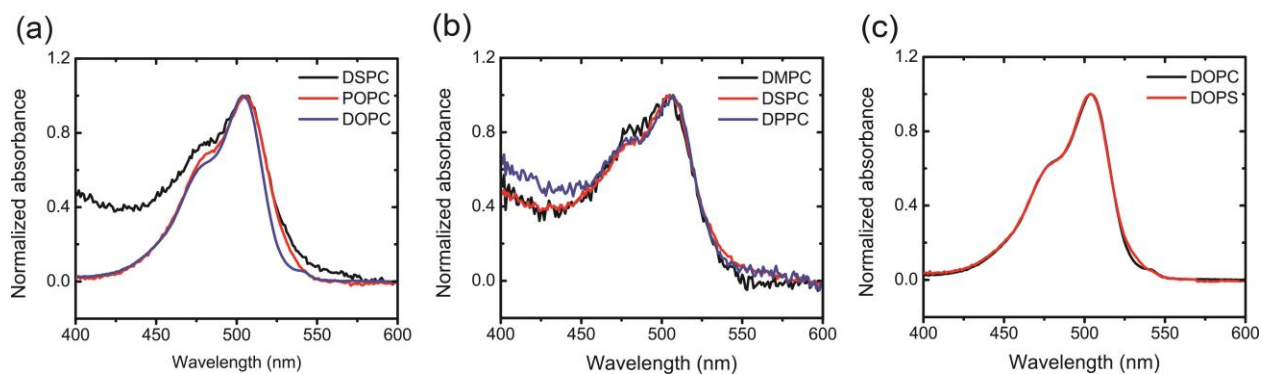


Figure S1. Normalized absorption spectra. The data was normalized to 0 at the absorbance value at 600 nm and to 1 for the peak absorbance value. (a) Acyl chain unsaturation. (b) Acyl chain length. (c) Lipid charge.

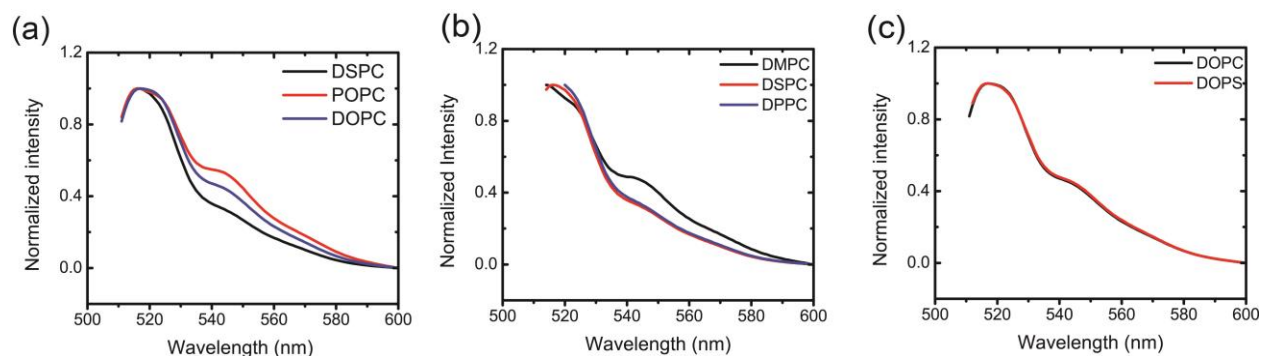


Figure S2. Normalized fluorescence emission spectra. The data was normalized to 0 for the emission value at 600 nm and to 1 for the peak emission value. (a) Acyl chain unsaturation. (b) Acyl chain length. (c) Lipid charge.

S2. Fluorescence decay curves and fits

TCSPC fluorescence decay curves were measured as described in the materials and methods section (section 2.6) of the manuscript. Representative decays are shown in Figure S3, while Table S2 gives the values for a double exponential fit of the decays, after normalizing the decays to 100 for $t = 0$ s.

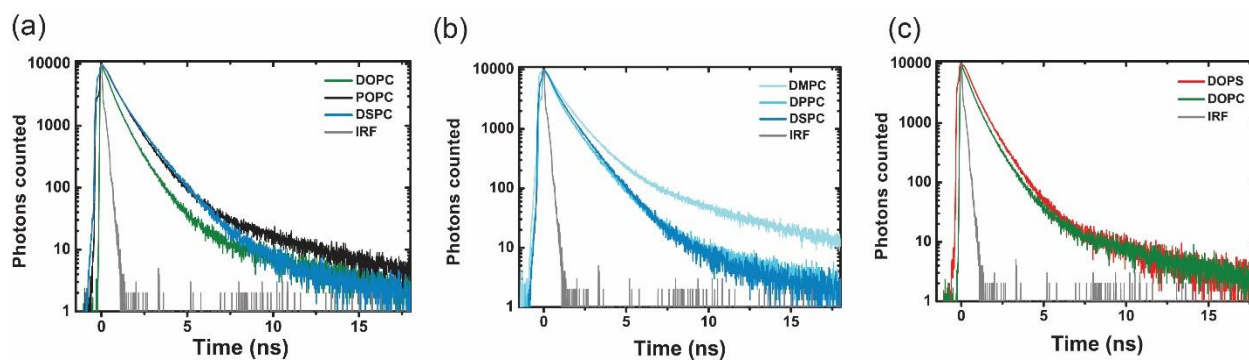


Figure S3. TCSPC fluorescence decay curves of SP-DiOC in LUVs of different compositions. Grey: instrument response function (IRF).

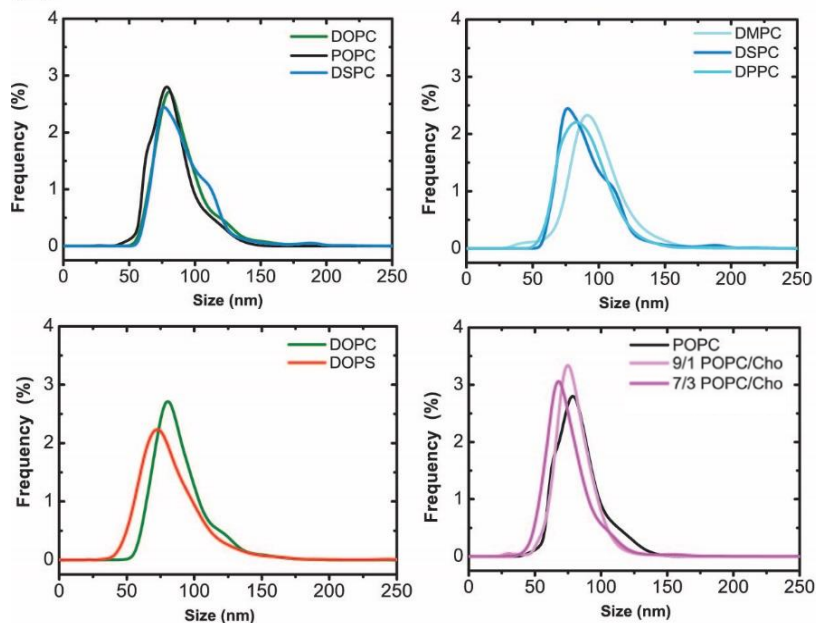
Table S2. Double-exponential fits of the TCSPC data. Life time (τ) is given in ps.

Formulation	τ_1	A1	τ_2	A2	Average τ
DOPS	663 \pm 100	88,6 \pm 9,8	1593 \pm 347	11,4 \pm 7,3	752 \pm 58
DOPC	528 \pm 2	80,8 \pm 0,6	1205 \pm 14	19,2 \pm 0,3	658 \pm 5
POPC	710 \pm 6	80,3 \pm 0,4	1509 \pm 128	19,7 \pm 5,2	861 \pm 4
DSPC	615 \pm 100	65,4 \pm 14,8	1450 \pm 190	34,6 \pm 11,7	892 \pm 48
DPPC	574 \pm 78	67,7 \pm 12,2	1427 \pm 202	32,3 \pm 8,6	831 \pm 37
DMPC	806 \pm 82	75,4 \pm 5,2	1852 \pm 76	24,6 \pm 4,8	1065 \pm 26
POPC/Chol 9/1	734 \pm 25	81,2 \pm 2,1	1924 \pm 280	18,8 \pm 1,3	951 \pm 52
POPC/Chol 7/3	504 \pm 34	86,3 \pm 2,9	1706 \pm 122	13,6 \pm 0,3	669 \pm 38

S3. Vesicle size distribution

The size distribution of all LUVs used in this study (Figure S4) were determined using nanoparticle tracking analysis as described in the materials and methods section (section 2.7) of the manuscript.

(a)



(b)

SUV Composition	Size mode (nm)	Distribution width (nm)	Total surface area (nm²)
DOPS	72 ± 3	42 ± 4	5.5E17 ± 0.2
DOPC	79 ± 2	18 ± 2	6.7E17 ± 0.5
POPC	72 ± 3	40 ± 7	3.0E17 ± 0.5
DSPC	73 ± 1	35 ± 5	2.3E17 ± 0.1
DPPC	80 ± 3	31 ± 2	2.0E17 ± 1.7
DMPC	84 ± 8	30 ± 6	6.0E17 ± 1.1
POPC/Chol 9/1	76 ± 3	29 ± 4	2.6E17 ± 0.3
POPC/Chol 7/3	73 ± 3	28 ± 4	1.2E17 ± 0.5

Figure S4. Vesicle sizes. (a) Size distributions of the vesicles used for this study as determined by nanoparticle tracking analysis. (b) Average sizes, distributions width (full width) and total surface area (TSA). Standard deviation (size mode, width distribution) and standard error of mean (TSA) are determined from the average of three independent vesicle batches.

S4. Separation of the free dye by size exclusion chromatography

After labeling the LUVs with SP-DiO, the free dye remaining in the solution was removed using spin-column size exclusion chromatography. Absorbance recordings of a control sample containing only dye, i.e. no LUVs, prior and after spin-column size exclusion chromatography showed that residual unbound dye was removed to a level below the detection limit by this procedure (Figure S5).

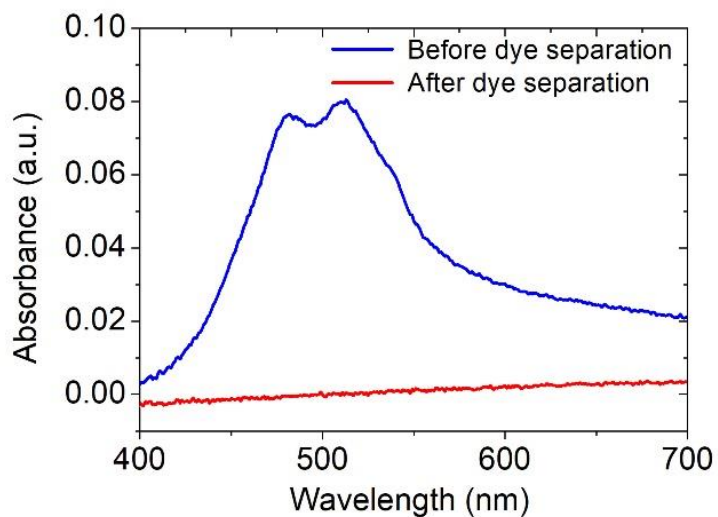


Figure S5. Dye separation by spin column size exclusion chromatography. Comparison of absorption of 40 μM SP-DiO in PBS before (blue) and after separation (red) of the dye.

S5. Dye-to-lipid ratio in stained LUVs

The LUVs were labeled by mixing dye and LUVs using a dye-to-lipid ratio of ~2%. The amount of incorporated dye and the resulting dye-to-lipid ratio (Table S1) was estimated from the absorbance data obtained in this work, using the Beer-Lambert Law and the molar extinction coefficient values presented in section S6. (For cholesterol containing membranes, the value for POPC was used). The total lipid content was then estimated from the total surface area, determined by particle concentration and size determination measurements using NTA (see section 2.7 in the materials and methods section of the main text). A lipid surface area of 0.8 nm² was assumed³⁷.

Table S3. Estimated dye/lipid ration in the various vesicle formulations used in this work.

Formulation	Dye/phospholipid ratio
DOPS	0.41%
DOPC	0.84%
POPC	0.36%
DSPC	0.14%
DPPC	0.05%
DMPC	0.04%
POPC/Chol 18%	0.34%
POPC/Chol 46%	0.87%

S6. Estimation of the molar extinction coefficients of SP-DiO in different lipid environments.

To provide a quantitative estimate of the value of the molar extinction coefficient of SP-DiO in different lipid environments, SP-DiO was incorporated into lipid membranes prior vesicle formation. To do so, 4 μ l of dye (225 μ M) in solvent (DMSO: Ethanol 1:1.25) were added to appropriate amounts of lipids in chloroform to obtain a molar dye-to-lipid ratio of 0.15%. The solvent was evaporated under a gentle nitrogen flow for at least 45 min. The lipid and dye mixture was then hydrated with 250 ml of PBS buffer, yielding a final lipid concentration of 2.4 mM. Hydration was performed at 70°C. For each sample a serial dilution series with dilution factor 2 was prepared (5 concentration, highest dye concentration: 0.9 mM) and 110 μ l were added to a transparent flat-bottom 96 well plate. Absorbance spectra were recorded between 400 and 600 nm using a multimode microplate reader Varioskan Flash (Thermo Fisher Scientific). To account for scattering due to the likely presence of large multilamellar vesicles, the data was baseline

corrected assuming a linear decay of the background scattering between 420 nm and 560 nm. The absorption peak value at 502 nm was measured. The data from two independent experiments was pooled together and plotted as absorbance versus concentration. For each vesicle type, a linear fit ($y=ax$) was applied. The molar extinction coefficient was calculated from the slope using the Beer Lambert law and an optical path length of 0.29 cm.

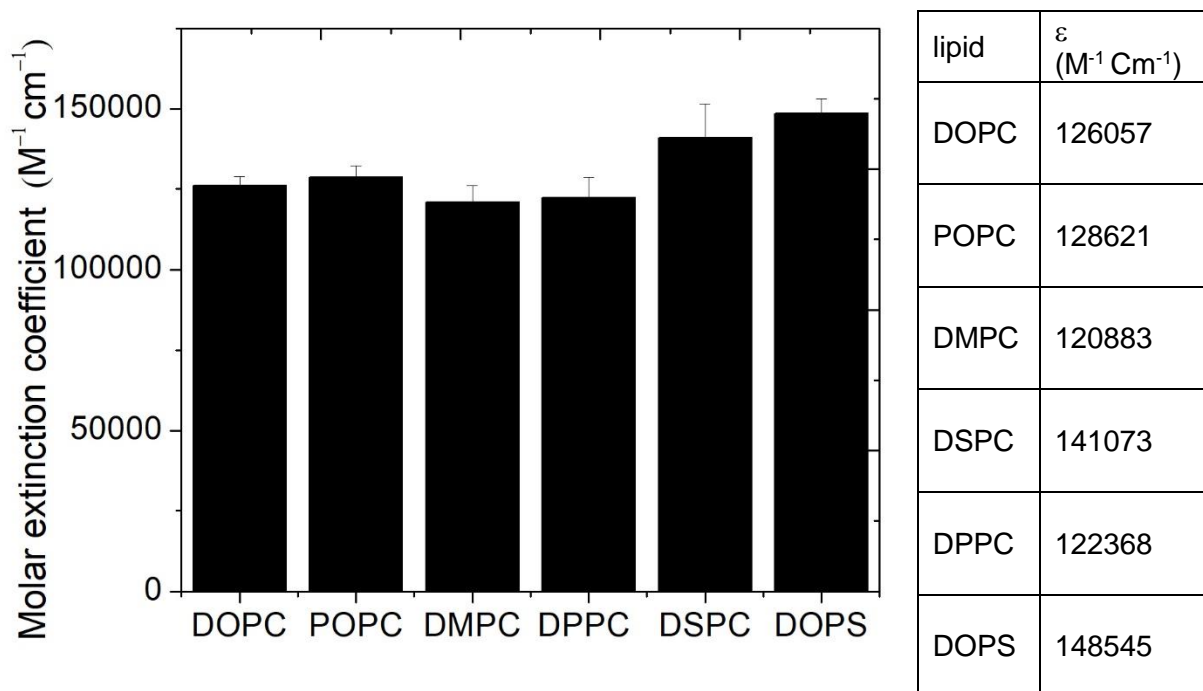


Figure S6. Estimated molar extinction coefficient of SP-DiO in different lipid environments. Error bars are the standard deviation of the linear fit.

S7. Labelling efficiency of DiO C18(3)

The labeling efficiency of the SP-DiO dye used in this study was compared to the one of DiO C18(3). Both dyes differ in that SP-DiO carries two sulfophenyl groups, improving dye solubility in aqueous environment and conferring the dye additional negative charges. To obtain the data shown in Figure S7, LUVs were labelled with the dye followed by absorption and fluorescence spectroscopy. Labeling and spectroscopy experiments were carried out as described in the manuscript. DiO was less efficient at producing strong fluorescent staining (Figure S7 a). Furthermore, it did not exhibit the same spectral shift in presence of cholesterol (figure S7 b), indicating that this very interesting feature of the SP-DiO dye is a unique feature due to the sulfophenyl group.

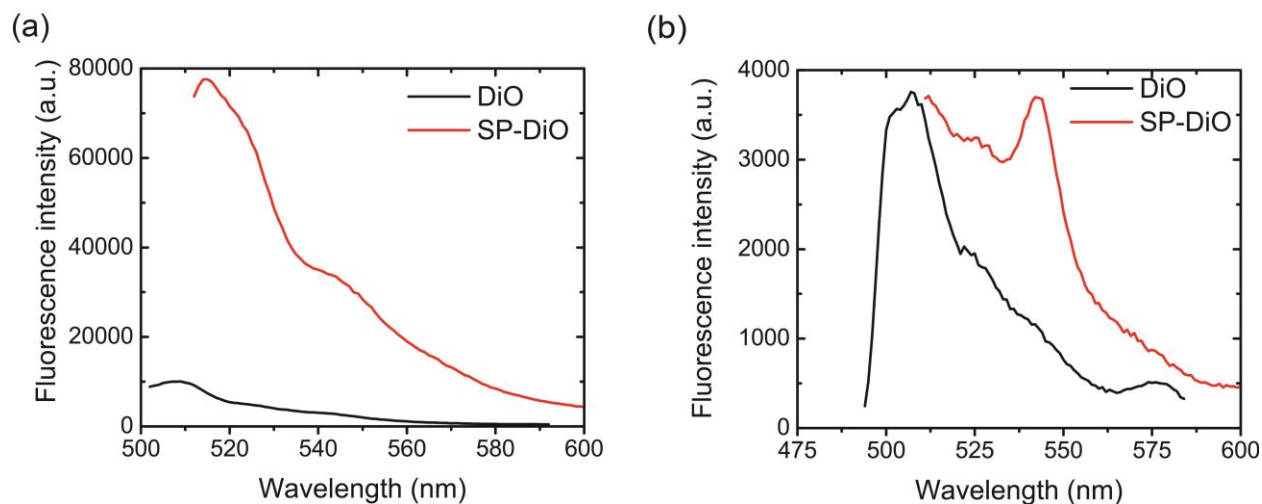


Figure S7. Labeling with DiO. (a) Comparison of the emission spectrum of POPC labelled with SP- DiO and DiO. Excitation wavelength: 492 nm (DiO) and 502 nm (SP-DiO). (b) Emission spectrum of POPC vesicle containing 46 mol% of cholesterol for DiO and SP-DiO. Excitation wavelength: 484 nm (DiO) and 501 nm (SP-DiO). DiO is shown in black and SP-DiO is shown in red.

S8. Changes of fluorescence spectra of cholesterol containing membranes upon consecutive exposure to light

The emission spectra of POPC vesicles and POPC vesicles containing cholesterol were recorded after consecutive exposure at 501 nm.

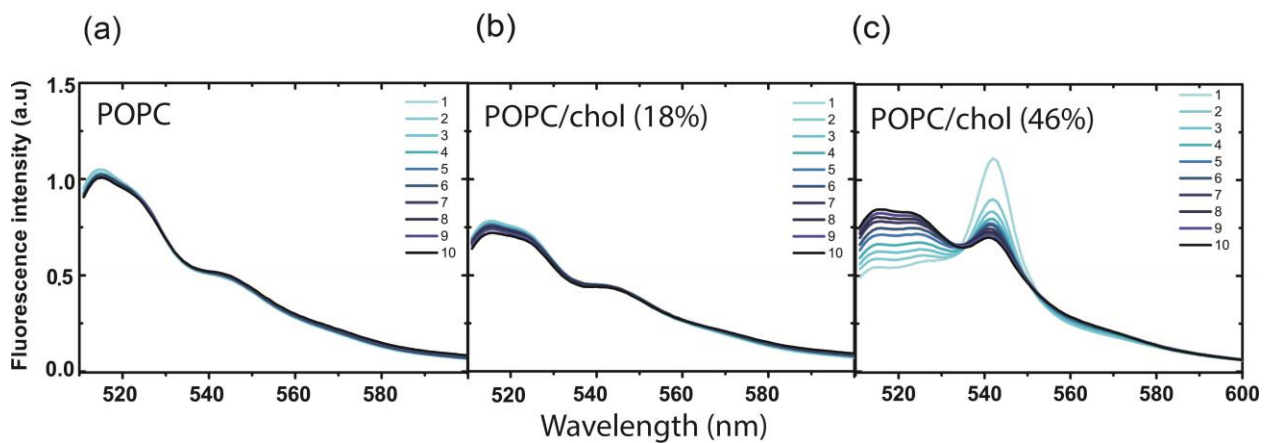


Figure S8. Fluorescence emission spectra of (a) POPC, (b) 18 mol % cholesterol in POPC and (c) 46 mol % cholesterol in POPC upon consecutive exposure at 501 nm.